Langmuir
Article
pubs.acs.org/Langmuir

Ultrafast Self-Assembly of Microscale Particles by Open-Channel Flow

Sun Choi,*[,†,‡,§] Inkyu Park,[∥] Zhao Hao,[§] Hoi-ying N. Holman,[§] Albert P. Pisano,[†,‡] and Tarek I. Zohdi[‡]

[†]*Berkeley Sensor and Actuator Center (BSAC),* [‡]*Department of Mechanical Engineering, and* [§]*Ecology Department, Earth Sciences Division, Lawrence Berkeley National Laboratory, University of California at Berkeley, Berkeley, California 94720, and* [∥]*Department of Mechanical Engineering, Korea Advanced Institute of Science and Technology (KAIST), 335 Gwahangno, Yuseong-gu, Daejon 305-701, South Korea*

Received September 15, 2009. Revised Manuscript Received October 29, 2009

We developed an ultrafast microfluidic approach to self-assemble microparticles in three dimensions by taking advantage of simple photolithography and capillary action of microparticle-dispersed suspensions. The theoretical principles of high-speed assembly have been explained, and the experimental verifications of the assembly of various sizes of silica microspheres and silica gel microspheres within thin and long open microchannels by using this approach have been demonstrated. We anticipate that the presented technique will be widely used in the semiconductor and Bio-MEMS (microelectromechanical systems) fields because it offers a fast way to control 3D microscale particle assemblies and also has superb compatibility with photolithography, which can lead to an easy integration of particle assembly with existing CMOS (complementary metal oxide−semiconductor) and MEMS fabrication processes.

Introduction

Microparticles are crucial building blocks for numerous applications such as bioassays,[1−4] photonics,[5,6] and microelectronic devices.[7,8] The self-assembly of microparticles is very favorable in microfabrication because it provides an easier, faster, and more convenient way to construct functional microstructures. A number of self-assembly techniques of microparticles have been developed on the basis of electrostatic force,[9] electrochemical reactions,[6,10] surface functionalization,[11] and microfluidics.[12−14] In particular, fluidic self-assembly is emerging as a promising pathway to guide and assemble microstructures because of its high yield and great simplicity.[15] It is reported that particles on the milimeter scale[16] and on the microscale[17] in fluids can be assembled and structured by lateral capillary forces between the particles in suspension, and the mechanism of the 2D crystallization of microparticles was also explained.[18] There have been several attempts to control 2D microparticle assembly from the liquid suspension of microparticles.[12,13,19−23] In particular cases, the assembly of the microparticles has been achieved in confined geometries by either a receding contact line[21,22] or electrostatic forces,[23] and the particles have been transported from the suspension to fill the trenches. These approaches require the fine control of the receding speed of the contact line and the contact angle of the meniscus of the fluid with respect to substrates. Also, the release of particle structure in the confined geometries, a crucial issue in the integration of on-chip particle assemblies with other microscale electronic devices, has not yet been demonstrated. Here, we describe a simple, ultrafast microfluidic approach to self-assemble microparticles in three dimensions on the basis of the photolithography and capillary action of microparticle-dispersed suspensions. Various sizes of silica microspheres and silica gel microspheres have been successfully assembled within open microchannels with a small cross-sectional area and a long length by using this approach. Also, microsphere-based line patterns have been fabricated by dissolving the photoresist that was used to guide the open-channel flow. In addition, the assembly speed has been estimated theoretically, and the discrepancy with experimental results has been discussed. The presented technique will provide a significant means to construct key structures in Bio-MEMS (microelectromechanical systems), chromatography on the microscale, 3D photonics, and various optical applications because it offers a convenient way to control the microparticle assembly with good compatibility with photolithography.

*To whom correspondence should be addressed. E-mail: sunchoi@eecs.berkeley.edu.

(1) Hänninen, P.; Soini, A.; Meltola, N.; Soini, J.; Soukka, J.; Soini, E. *Nat. Biotechnol.* **2000**, *18*, 548–550.
(2) Lilliehorn, T.; Nilsson, M.; Simu, U.; Johansson, S.; Almqvist, M.; Nilsson, J.; Laurell, T. *Sens. Actuators, B* **2005**, *106*, 851–858.
(3) Nie, Q.; Zhang, Y.; Zhang, J.; Zhang, M. *J. Mater. Chem* **2006**, *16*, 546–549.
(4) Bayerl, T. M. *Nature* **2004**, *427*, 105–106.
(5) Rinne, S. A.; Garcia-Santamara, F.; Braun, P. V. *Nature* **2007**, *2*, 52–56.
(6) Braun, P. V.; Wiltzius, P. *Nature* **1999**, *402*, 603–604.
(7) Gracias, D. H.; Tien, J.; Breen, T. L.; Hsu, C.; Whitesides, G. M. *Science* **2000**, *289*, 1170–1172.
(8) Mezzenga, R.; Ruokolainen, J.; Fredrickson, G. H.; Kramer, D. M.; Heeger, A. J.; Ikkala, O. *Science* **2003**, *299*, 1871–1874.
(9) Grzybowski, B. A.; Winkleman, A.; Wiles, J. A.; Brumer, Y.; Whitesides, G. M. *Nat. Mater.* **2003**, *2*, 241–245.
(10) Walcarius, A.; Sinottier, E.; Etienne, M.; Ghanbaja, J. *Nat. Mater.* **2007**, *6*, 602–608.
(11) Qin, D.; Xia, Y; Xu, B.; Yang, H.; Zhu, C.; Whitesides, G. M. *Adv. Mater.* **1999**, *11*, 1433–1437.
(12) Kim, E.; Xia, Y.; Whitesides, G. M. *Adv. Mater.* **1996**, *8*, 245–247.
(13) Dushkin, C. D.; Yoshimura, H; Nagayama, K. *Chem. Phys. Lett.* **1993**, *204*, 455.
(14) Fialkowski, M.; Bitner, A.; Grzybowski, B. A. *Nat. Mater.* **2005**, *4*, 93–97.
(15) Chung, S. E.; Park, W.; Shin, S.; Lee, S. A.; Kwon, S. *Nat. Mater.* **2008**, *7*, 581–587.
(16) Bowden, N.; Terfort, A.; Carbeck, J.; Whitesides, G. M. *Science* **1997**, *276*, 233–235.
(17) Denkov, N. D.; Velev, O. D.; Kralchevsky, P. A.; Ivanov, I. B.; Yoshimura, H.; Nagayama, K. *Nature* **1993**, *361*, 26.
(18) Denkov, N. D.; Velev, O. D.; Kralchevsky, P. A.; Ivanov, I. B.; Yoshimura, H.; Nagayama, K. *Langmuir* **1992**, *8*, 3183–3190.
(19) Dimitrov, A. S.; Nagayama, K. *Langmuir* **1996**, *12*, 1303–1311.
(20) Yamaki, M.; Higo, J.; Nagayama, K. *Langmuir* **1995**, *11*, 2975–2978.
(21) Yin, Y.; Lu, Y.; Gates, B.; Younan Xia, Y. *J. Am. Chem. Soc.* **2001**, *123*, 8718–8729.
(22) Su, G.; Guo, Q.; Palmer, R. E. *Langmuir* **2003**, *19*, 9669–9671.
(23) Golding, R. K.; Lewis, P. C.; Kumacheva, E.; Allard, M.; Sargent, E. H. *Langmuir* **2004**, *20*, 1414–1419.

Experimental Methods

Materials. A liquid suspension of silica microspheres (silicon dioxide-based microparticles; diameter, 3 and 5 μm; water, 95 wt %; silica, 5 wt %, Sigma-Aldrich) has been diluted into various concentrations of suspension (2.5, 1.25, 0.625, and 0.3125 wt % silica) by adding a controlled volume of deionized water. Dried silica gel spheres with a diameter of 3 μm, a pore size of 6 nm, and a distribution of diameters (D10, 2.15 μm; D50, 3.40 μm; and D90, 6.42 μm) (SiliaSphere, Silicycle) were mixed with a controlled volume of deionized water to form suspension of 1.25 wt % silica gel and 98.75 wt % water.

Design and Fabrication of Open Microchannels. Two reservoirs and the channel geometry were designed. For inlet/outlet reservoirs, 20 mm × 20 mm × 7 μm (width × length × height) rectangular patterns were defined to contain a 0.2 μL volume of suspension without overflow. For channels, various widths (10, 13, 16, 20, 40, and 60 μm) and lengths (2, 3, 4, 5, 6, 7, and 8 mm) have been combined with fixed height (7 μm). The open microchannel has been fabricated by UV photolithography. Lightly doped p-type silicon wafer (Silicon Quest International Inc.) was used as a substrate, and SU-8 2007 (Microchem Corp.) and SPR 220-7 (Megaposit) were used as UV-sensitive photoresists. For the SU-8 channel, the resist was spin coated onto a silicon substrate at 3000 rpm for 30 s (thickness ~7 μm) and soft baked at 95 °C for 3 min. After UV-light exposure, the sample was baked at 95 °C for 3 min for a postexposure bake and developed for 1 min. For SPR 220-7 channels, the resist was spin coated onto a silicon substrate at 2200 rpm for 30 s (thickness ~10 μm) and soft baked at 115 °C for 5 min. After UV-light exposure, the sample was developed for 4 min. After the lithography step, oxygen plasma treatment (50 W, 260 mTorr, 30 s) enhanced the hydrophilicity of the channel wall and substrate.

Patterning of Microparticles. All the patterning experiments on the open microchannel were conducted in an air environment at atmospheric pressure and room temperature. A microsyringe (Microliter Syringes 5 μL, Hamilton) was used to extract a small volume (0.2 μL) of the microparticle solution in the inlet reservoir. After the particle assembly was completed, the sample was held at room temperature for 1 h to evaporate the solvent completely and the resist was dissolved by PRS 3000 (J. T. Baker) in case of the SPR 220-7 micro-open channel.

Imaging. The samples were imaged by optical microscopy (Polylite 88, Reichert-Jung) and scanning electron microscopy (LEO 1550, Zeiss). A cross section of the channel was imaged after the sample was coated via the sputtering of a Au/Pd thin film.

Principles of the Self-Assembly of Microparticles

Figure 1 illustrates the sequential processes of self-assembly in the open microchannel. The self-assembly of microparticles in the micro-open channel is divided into three steps: (1) initiation of particle nucleation (scheme 1c); (2) crystal growth of the particle nucleus (scheme 1d); and (3) completion of crystal growth followed by medium evaporation (scheme 1e,f). The capillary immersion force generates a strong attractive force between the particles when the fluid thickness reaches the particle diameter (D) if $D \leq 5$ μm.[24] If the capillary pressure from the suspension droplet is sufficient to be maintained throughout the channel, then the medium is driven by the surface tension of the channel and flows along the channel. The thickness of the medium film sharply decreases at the interface between the channel and the outlet because of the divergence of medium flow. Then, the particles are attracted to each other and nucleated at the interface. After the onset of particle nucleation, a convective flux of particles from the channel inlet to the ordered particle nucleus propagates the particle assembly by crystal growth.

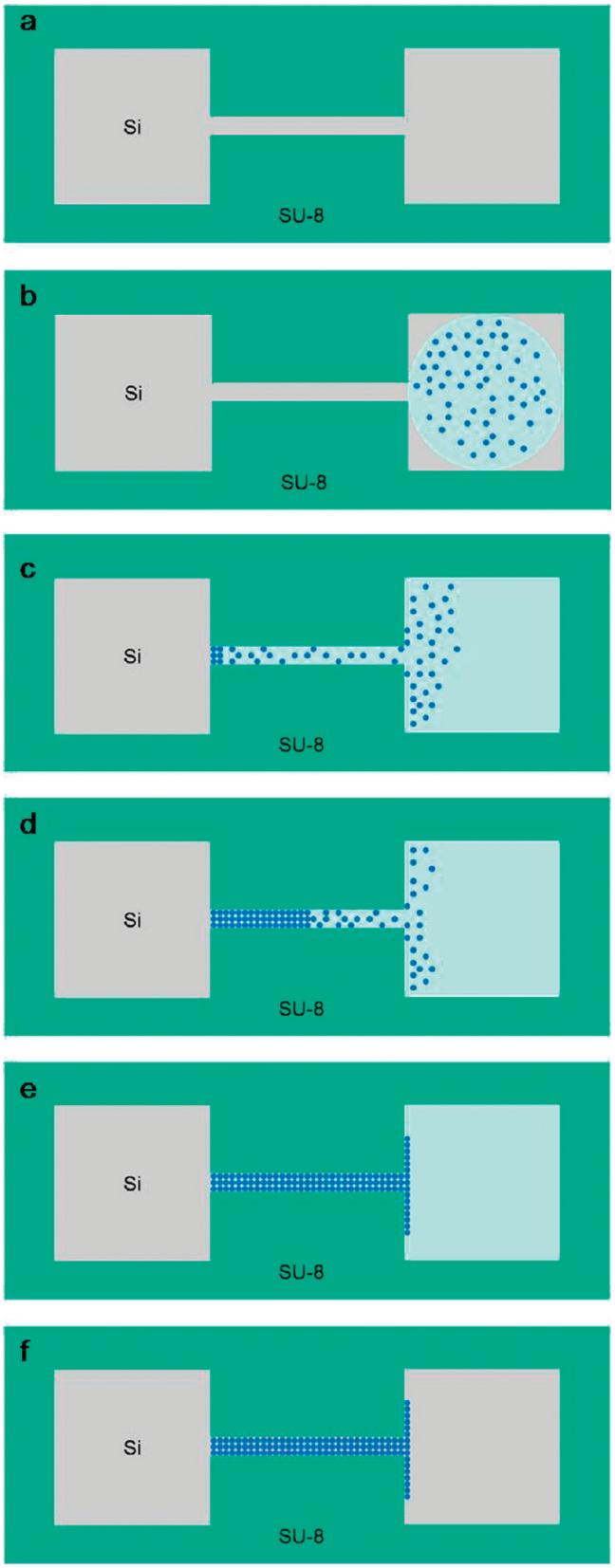

Figure 1. Schematics of the self-assembly of the microparticles in a microopen channel. (a) SU-8 micro-open channel fabricated on the silicon substrate. (b) Microparticle-dispersed suspension placed on the inlet of the micro-open channel. (c) The suspension is driven by the surface tension, and the particles stop at the interface between the channel and outlet and crystallization starts. (d) Particle crystallization develops. (e) Crystallization is completed. (f) Medium is evaporated.

(24) Kralchevsky, P. A.; Denkov, N. D. *Curr. Opin. Colloid Interface Sci.* **2001**, *6*, 383–401.

The convective flux of particles is generated by two sources: evaporation of the medium and capillary action of the medium. The evaporation of the medium occurs rapidly at the particle nucleus where menisci of the medium are formed around the particles. These menisci prevent the further thinning of the medium layer in the nucleus, and an intensive medium flux from the thicker part of the medium layer is generated to compensate for medium evaporation at the nucleus.[17] The capillary action of the medium is caused by the Young−Laplace capillary pressure on the microscale. The high surface tension of the substrate and sidewall of channels, after O_2 plasma treatment, can induce a high medium flux from a droplet in the channel inlet in the microscale open channel. Therefore, the medium flux by both the evaporation of the medium at the nucleus and the capillary pressure of the medium carries the suspended particles toward the nucleus and results in fast particle assembly. (The assembly time is 24 s in an open microchannel where the width is 20 μm, the height is 7 μm, and the length is 4 mm. See the figures in Supporting Information.) After the nucleus is propagated to the inlet of the channel, the medium in the nucleus evaporates completely and particle assembly is completed within defined microchannel geometries.

Theoretical Calculations

The crystal-growth rate of particle assembly can be theoretically estimated by combining the model of convective assembly of colloid particles[19] with the open-channel flow model.[25] On the basis of Dimitrov's model,[18] the crystal-growth rate of convective particle assembly at steady state, v_c, is expressed in terms of the macroscopic mean velocity of water, v_{wt}, mean evaporative flux of the medium from assembled particles, j_e, medium film thickness, h, leading edge of medium thickness, h_f, distance between the leading edge of the medium film and inlet reservoir, l, porosity of particle assembly, ε and volume fraction of particles in suspension, Φ.

$$v_c = \frac{\beta h_f v_{wt} \phi}{h(1-\varepsilon)} = \frac{\beta j_e l \phi}{h(1-\varepsilon)(1-\phi)} \quad (1)$$

The mean evaporative flux of the medium from assembled particles, j_e, is defined as $(\int_0^\infty j_e(z)\,dz/l)$ where z refers to the axis of propagation of particle assembly and β is the coefficient that depends on the particle−particle and particle−substrate interactions and varies from 0 to 1. If the interactions are stronger, then the value of β increases. For nonadsorbing particles such as silica particles or diluted suspensions, β approaches 1. As mentioned above, the medium flow in an open channel is mainly driven by two sources: capillary flow driven by surface tension and enhanced evaporation of water by the meniscus effect in particle assembly. Because it is difficult to measure j_e experimentally, another strategy has been assessed to quantify the contribution of capillary channel flow to the enhancement of the crystal-growth rate. v_c at the interface between the outlet and channel is theoretically estimated on the basis of the assumption that the capillary flow is the only source to drive water flow inside the channel. The volume flow rate of water in the open channel, Q, by capillary pressure only is expressed as[25]

$$Q = \frac{1\Delta P}{\eta R_{fr}} \quad (2)$$

$$R_{fr} = \frac{12L}{R_h{}^2 A}(1 - 1.3553a + 1.9467a^2 - 1.7012a^3 + 0.9564a^4 - 0.2537a^5) \quad (3)$$

where η is the viscosity of the liquid, ΔP is the difference of pressure between the two liquid fronts, L is the filled length of the channel, R_h is the hydraulic radius of the channel, A is the cross-sectional area of the channel, and a is the aspect ratio of the channel. The aspect ratio is defined as either height/width or width/height such that $0 \le a \le 1$. The capillary pressure that is equivalent to ΔP in the flow direction (z) of the open microchannel can be described as[25]

$$P_{c,z} = \gamma\left(\frac{\cos\alpha_b}{d} + \frac{\cos\alpha_l + \cos\alpha_r}{w}\right) \quad (4)$$

where γ is the surface tension of a liquid and α_b, α_l, and α_r are the contact angles of the liquid on the bottom, left, and right walls, respectively. d and w are the depth and width of a microchannel.

Therefore, v_{wt} and v_c by the capillary flow of water is

$$v_{wt\_capillary} = \frac{1}{\eta A}\frac{P_{c,z}}{R_{fr}} \quad (5)$$

$$v_{c\_capillary} = \frac{\beta h_f v_{wt\_capillary}\phi}{h(1-\varepsilon)} \quad (6)$$

It is important to note that the estimated $v_{c\_capillary}$, according to the formulations above, is valid mainly at the interface between the channel and outlet. The natural evaporation of water in a suspension droplet in the inlet reservoir increases the concentration of solutes in the suspension as crystal growth proceeds. However, this effect was not included in the formulation. Also, the loss of a pressure gradient caused by crystallized columns was not considered in the formulations. We denote $v_{c\_capillary}$ as v_c in this article for simplicity. We will discuss the discrepancy between the theoretically estimated v_c and the measured v_c in the Results and Discussion section.

Results and Discussion

Commensurable Effect. Figure 2 shows that the silica microspheres are assembled tightly within the microopen channel in three directions: horizontal (x axis) and vertical (y axis) directions in the plane of the channel cross section and in the direction of the channel length (z axis) by using the presented technique. The crystal growth of particles after the initial nucleation is governed by forces in three directions: horizontal and vertical by the evaporation of the medium and in the direction of the channel by the capillary action of the medium. Also, the interface between the channel and outlet reservoir has been sharply defined, and no particle overflow is found, which is consistent with the claim that the nucleation of particles begins where the thickness of the water film is reduced to the particle diameter. The commensurable effect of silica microspheres in the open microchannel is examined in more detail by varying the width of the channel and the diameter of silica particles. At first, the number of particles across the channel width is increased by one as the width of the channel increased by the particle diameter. Because the assembly of particles is achieved to minimize the porosity, the number of complete particles across the width ($= N_1$) is equal to [W(width)/D(particle diameter)], where function [x] returns the largest integer less than or equal to x. It turns out that the number of particles across the channel height decreased as the channel aspect ratio (H(channel height)/w(channel width)) decreased, although we anticipated that the number of particles ($= N_2$) across the channel would be the same as [H(height)/D(particle diameter)]

(25) Ryu, W. A.; Huang, Z.; Park, J. S.; Moseley, J.; Grossman, A. R. *Lab Chip* **2008**, *8*, 1460–1467.

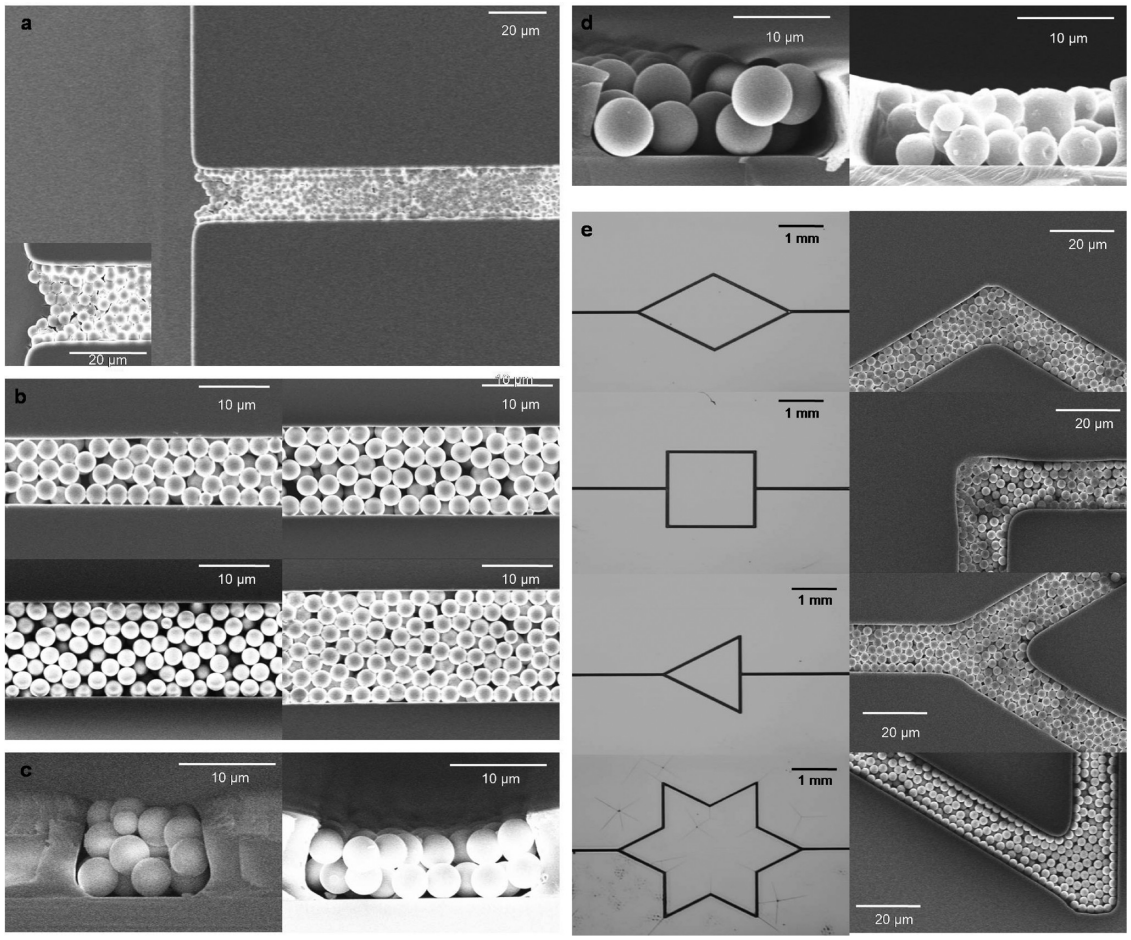

Figure 2. SEM images of the assembly of 3-μm -diameter silica microspheres within the SU-8 micro-open channel. (a) Interface between the channel and outlet reservoir. The channel width is 20 μm, the height is 7 μm, and the length is 4 mm. The outlet reservoir is 2 mm $\times$ 2 mm $\times$ 7 μm (height). (b) Commensurable effect of silica microspheres on a horizontal scale. The widths of the channels are 10 μm (top left), 13 μm (top right), 16 μm (bottom left), and 20 μm (bottom right). The length (3 mm) and height (7 μm) of four microchannels are identical. The numbers of particle layers are three (top left), four (top right), five (bottom left), and six (bottom right). (c) Commensurable effect of 3 μm silica microspheres on a vertical scale. (d) Cross-sectional view of 5 μm silica microspheres (left) and 3 μm silica gel microspheres (right). The widths of the channels are 20 μm (right). (e) Optical microscope (left column) and SEM (right column) images of assembled silica microsphere structures in rhombus-shaped (top), square-shaped (upper middle), triangle-shaped (lower middle), and star-shaped (bottom) channels. The SEM images in the right column represent particle assemblies at the diverted paths of channels.

regardless of the channel widths. It is speculated that the geometry of the interface between the suspension and air affects the nature of self-assembly. Inside the channel with a lower aspect ratio, a thinner-medium film is formed because the contact angle of water with respect to the channel sidewall remains constant even if the channel width changes. Consequently, a thinner-medium film carries and assembles fewer particles on the vertical scale. Therefore, not only the height of the channel but also the geometry of suspension interface with air determine the number of silica layers on the vertical scale. When the size of the microspheres is increased from 3 to 5 μm, the number of particles on both the horizontal and vertical scales was decreased.

Silica gel microspheres that are widely used materials in conventional chromatography have been self-assembled by using the presented technique. The solid-state silica gel particles are diluted with the medium, and a droplet of the acquired suspension is applied to the channel. Although silica gel particles show a wider distribution of diameters and have water-absorbing properties, the interface between the assembled structures and outlet reservoir has been clearly defined and the particles have been assembled tightly, as can be seen from Figure 1. It shows that particle assembly occurs in both the vertical and horizontal directions with respect to the channel width simultaneously, not sequentially. It is noteworthy that various microparticles can be self-assembled according to the channel geometry because the pathway and the height of the fluid-state medium determine the 3D geometry of the assembled structure. The 3D assembly of microparticles can be easily structured within a micro-open channel whose geometry can be easily controlled by a photolithographic processes. The self-assembly of microparticles in various geometries has also been demonstrated in Figure 1e.

Theoretical Analysis. We have obtained data on the length of crystal growth versus time by taking snapshots of the crystallization of silica microspheres in open microchannels with an optical microscope. Detailed data are available in Tables 1 and 2 in Supporting Information. We have calculated the theoretically estimated length of crystal growth based on the model provided in the previous section. First, we calculated the crystal-growth rate, v_c, and integrated it to obtain the length of crystal growth, L_c. Also, we have obtained the relation between the weight fraction of particles in a liquid suspension and v_c, and we have observed the discrepancy between the measured and estimated v_c. As shown in Figure 2, the theoretically estimated and measured L_c values are similar to each other at the beginning of crystallization;

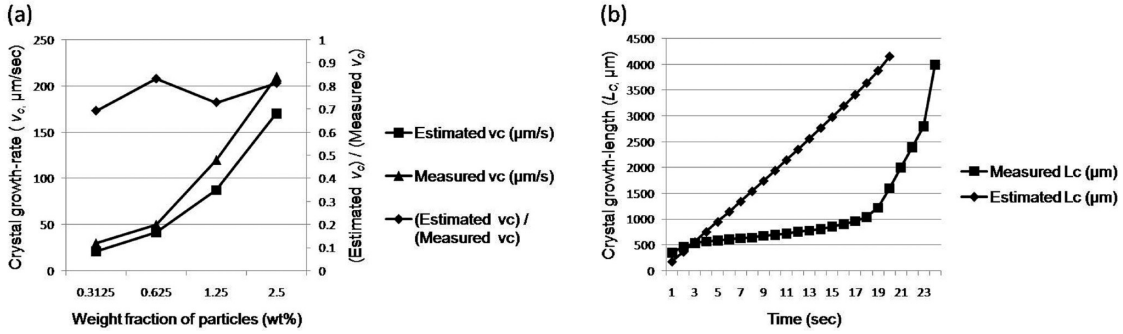

Figure 3. Graphs of the crystal growth length (L_c) versus time (left) and the crystal growth rate (v_c) and the ratio of estimated to measured v_c versus the weight fraction of particles (right).

however, they start to show larger discrepancy later on. The slope of the graph indicates that v_c changes drastically from lower to higher in the middle of crystallization in the measured L_c, and the estimated L_c shows the trend of a linear increase until the completion of crystallization. Because of the rapid increase in measured v_c, the overall times required for crystallization for both the theoretical estimation and experiments are similar although the dynamics of v_c is different during the crystallization. The discrepancy between estimated and measured L_c is attributed to the effects of natural evaporation of droplets and the loss of a pressure gradient caused by the crystallized column. The significant decrease in measured v_c after initial crystallization is caused by the effect of the loss of the pressure gradient. This loss increases as the crystallization proceeds, thus v_c also decreases. Although the loss of the pressure gradient increases until the completion of crystallization, because of the natural evaporation of the medium in suspension the concentration of particles in suspension increases and v_c increases. The significant uproar concerning v_c is caused by the nonlinear nature of the evaporation of the medium. Although we do not quantitatively characterize the evaporative power of the medium in a suspension droplet with respect to time, we are able to observe that the evaporative rate increases drastically as the droplet evaporates because the surface-to-volume ratio of a single droplet also increases. Therefore, we speculate that this nonlinear increase in the evaporative power of the medium in the suspension droplet drives the significant increase in v_c in spite of the larger loss of the pressure gradient in the late stage of crystallization. As stated in Theoretical Calculations, the effects of the natural evaporation of a droplet and the loss of the pressure gradient caused by the crystallized column are not considered in the theoretical modeling; therefore, the discrepancy between the estimated and measured L_c values is observed in the middle of the crystallization. However, in an early stage of crystallization when the crystallized particles dwell at the interface between the outlet reservoir and channel, the estimated v_c agrees well with the measured one because the pressure loss caused by the crystallized column is not large and the evaporative rate of the droplet is also negligible. The ratio of the estimated to measured v_c was calculated at the point where the first two snapshots of crystallization are taken. It is maintained at about 0.7−0.8 throughout all of the fractions of particles, implying that the theoretical model is valid around the interface between the outlet reservoir and the channel and also that the contribution of capillary action of flow to crystal growth is more dominant than the evaporation of the medium at the interface. Therefore, we conclude that the surface treatment of the channel by oxygen plasma is very critical to achieving the high-speed crystallization of particles in an open microchannel.

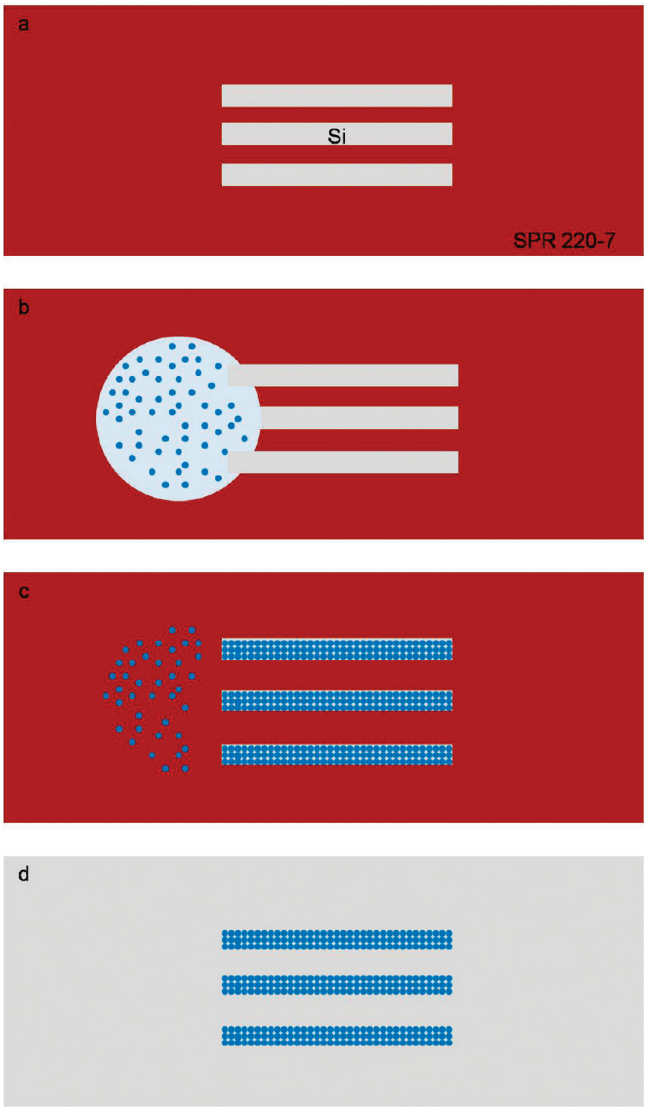

Figure 4. Fabrication of microparticle self-supported line patterns based on microspheres. (a) Multiple (or single) lines are patterned onto the photoresist. (b) Droplets of the liquid suspension are placed on one end of the channel. (c) Particles are assembled inside the line patterns. (d) The photoresist is dissolved, and a particle assembly is formed.

Release of Particle Assembly. Self-supported line patterns based on the assembly of silica microspheres have been fabricated by flowing silica suspension in the photoresist-based open channel and subsequent removal of the photoresist by solvent. A thick

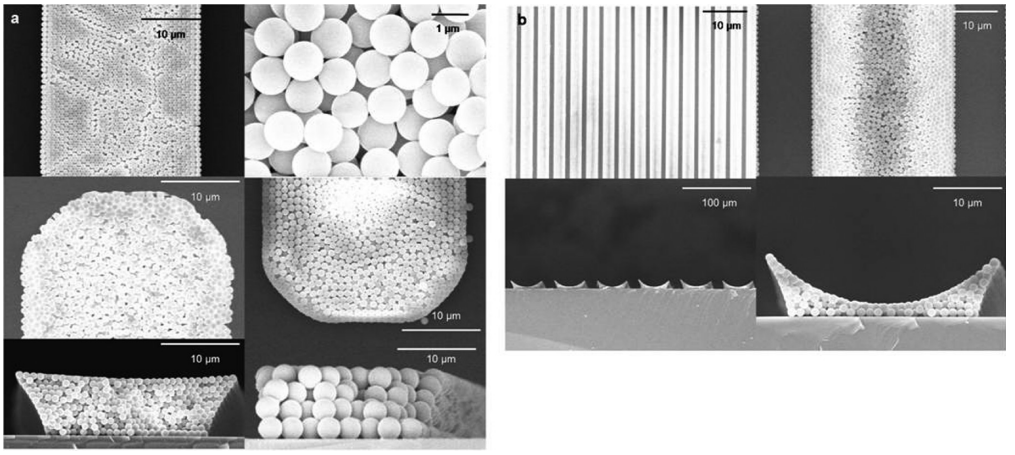

Figure 5. SEM images of self-supported line patterns based on silica microspheres. (a) Line patterns generated by a single channel. (Center, Top Left) Close view of assembled particles (top right), front end (middle left), bottom end (middle right), cross-sectional views of a 1 μm silica microsphere-based line (low left), and cross section view of 3 μm silica microspheres (low right). The length (4 mm) and width (20 μm) of channels and volume of a droplet (0.2 μL) are fixed. (b) Line patterns generated by multichannels based on 1 μm silica microspheres. Top view of the overall pattern (top left) and magnified view (top right) of the line patterns. Cross-sectional view of the overall (lower left) and individual lines (lower right).

photoresist (SPR 220-7, MEGAPOSIT, depth ~10 μm) is used to define the channel geometry, and it is dissolved by nonpolar solvent (PRS 3000, J. T. Baker) after the particle assembly is completed. Single and multichannel patterns have been used in this patterning. Both ends of the open microchannel are designed to be closed in order to prevent the flow in one channel from being disturbed by the outflows from other channels. The droplet is placed at one end of the channels as shown in Figure 4.

In spite of the expected higher flow resistance at the end of the channels, close packing of particles is achieved over the entire length of lines as shown in Figure 3. It was also observed that the crystallization of particles starts at the end of the channel in the case of a closed channel, which is observed in an open channel as well. Once the medium reaches the end of the channel, the thickness of the medium is forced to decrease in order to satisfy the continuity of fluid. This significant decrease in the flow starts at the end of channel, thus the crystallization also begins there. The particles are completely filled from the front end of the channel—the furthest point from the droplet—to the rear end of the channel, inside the droplet, without any depletion of particles. It is noteworthy that the packing structure can be preserved without any perturbation during the removal process of the photoresist. The assembled structure is preserved until the diameter of silica microspheres reaches 3 μm; however, the structure is perturbed when the diameter is 5 μm. If the particle size decreases, then the surface-to-volume ratio and the contact area increase, thus a stronger van der Waals force may preserve the particle assembly intact. Also, the surface charge condition of particles is another crucial factor in the stability of the structures. The microstructure based on polystyrene microspheres (diameter ~1 μm) is deteriorated after the photoresist removal. From these observations, one can conclude that the interparticle forces of assembled structure are dependent on the surface charge property of particles as well. Negatively charged colloidal particles, such as polystyrene, cannot withstand the resist-removal process because the interparticle electrostatic repulsion force is stronger than the attractive force in nonpolar solvents.[26] It is anticipated that the smaller, insulating, or semiconducting particles will be more advantageous in line patterning than the larger and metallic particles. Another interesting feature is the dependence of pattern shape on the number of microchannels when the same volume of microparticle suspension is used. Whereas a meniscus effect of the fluid−channel wall interface is not observed in the patterning of single channels, a huge meniscus effect is found in the multichannel patterning and the thickness of the pattern at the center of the channel is decreasing. This dependence is caused by the difference in capillary pressure at the inlet. In single channels, the dispensing port has a relatively large wetted perimeter compared to the microchannels and the driving pressure is equal to the capillary pressure between two liquid fronts as discussed previously.[25] However, in multichannels, the perimeter of the suspension droplet per channel is not as sufficient as that for a single-channel case, thus resulting in the decrease in capillary pressure. Therefore, a thinner medium flow will be established, and this flow drives fewer particles and forms a thinner particle assembly. This patterning process is expected to be easily extended to multilayer processes and integrated with other IC processes because the geometry of the assembly can be easily tuned by setting the resist thickness and channel features, and an accurate alignment can be achieved.

Conclusions

We have demonstrated the ultrafast assembly of microparticles by using simple photolithography and the surface-tension-induced capillary action of a microparticle dispersed suspension. High-speed assembly of silica and silica gel microparticles has been achieved within a thin, long, open microchannel, and this phenomenon has been modeled and compared with experimental data. The commensurable effect of assembled particles within the channels is addressed, and self-supported particle-based patterns have been fabricated by dissolving the photoresist. Thanks to its simplicity, compatibility with IC (integrated circuits) processes and wide applicability to various types of particles and substrates, we expect that this presented technique will be widely used in various applications such as chromatography and microfilters in on-chip bioassay, microstructures on cell chips, and tunable 3D photonic crystals for waveguide and microcavity structures.

Acknowledgment. This research is supported by the U.S. Department of Energy (DOE, grant no. DE-AC02-05CH112) and a grant (2009K000069) from the Center for Nanoscale Mechatronics & Manufacturing (CNMM), one of the 21st Century Frontier

(26) Sainis, S. K.; Germain, V.; Mejean, C. O.; Dufresne, E. R. *Langmuir* **2008**, *24*, 1160–1164.

Research Programs, which are supported by the Ministry of Education, Science and Technology, Korea. S.C. is grateful for a graduate fellowship from the Samsung Scholarship Foundation, and I.P. is grateful for partial support from the National Research Foundation grant funded by the Korea government (MEST) (No. 2009-0082529).

Supporting Information Available: Series of snapshots describing the nature of particle assembly in a micro-open channel. Detailed data on the theoretically estimated and measured length of crystal growth and rate of growth. This material is available free of charge via the Internet at http://pubs.acs.org.